

2013

The Mechanism of Photo-Hydrosilylation on Silicon and Porous Silicon Surfaces

Kurt W. Kolasinski

West Chester University of Pennsylvania, kkolasinski@wcupa.edu

Follow this and additional works at: http://digitalcommons.wcupa.edu/chem_facpub



Part of the [Materials Chemistry Commons](#)

Recommended Citation

Kolasinski, K. W. (2013). The Mechanism of Photo-Hydrosilylation on Silicon and Porous Silicon Surfaces. *Journal of the American Chemical Society*, 135(30), 11408-11412. Retrieved from http://digitalcommons.wcupa.edu/chem_facpub/6

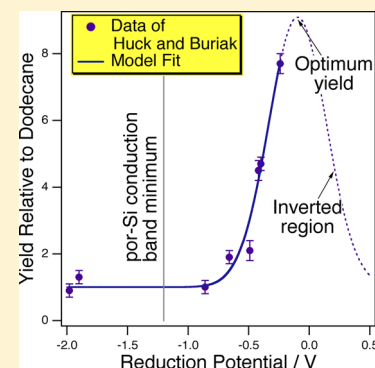
This Article is brought to you for free and open access by the College of Arts & Sciences at Digital Commons @ West Chester University. It has been accepted for inclusion in Chemistry by an authorized administrator of Digital Commons @ West Chester University. For more information, please contact wcressler@wcupa.edu.

1 The Mechanism of Photohydrosilylation on Silicon and Porous 2 Silicon Surfaces

3 Kurt W. Kolasinski*

4 Department of Chemistry, West Chester University, West Chester, Pennsylvania 19383, United States

5 **ABSTRACT:** Visible or UV light activates H-terminated Si surfaces because of the
6 presence of a photogenerated hole in a Si–Si back-bond. Enhancing the lifetime of this
7 hole at the surface increases reactivity. On the basis of photodynamics and electron transfer
8 theory, the prevalence of two mechanisms of photoactivation (internal photoemission
9 versus interband photoexcitation followed by electron transfer) are explored. To act as an
10 effective trap, an acceptor state for the excited electron must either be populated directly by
11 photoexcitation or the state must lie in a band gap (or both). It is predicted that oxidants
12 with a properly positioned acceptor level will enhance the reactivity of porous silicon or
13 silicon nanocrystals in a size selective manner.



14 ■ INTRODUCTION

15 The ability to tune the solubility, wettability, and dissolution
16 behavior of nanocrystalline silicon (nc-Si) by variations in
17 surface termination makes porous silicon (por-Si) an ideal
18 vehicle for drug delivery.^{1–3} Silicon nanoparticles exhibit
19 improved solubility in polar solvents when longer alkyl chains
20 are attached to them.⁴ Carboxylic acid-terminated Si nano-
21 particles do not exhibit cytotoxicity, whereas amine-terminated
22 Si nanoparticles do.⁵ H-terminated surface are easily
23 resorbed,^{6,7} whereas derivatization can inhibit the corrosion
24 of por-Si surfaces.⁸ Decelerated dissolution can slow the release
25 of a steroid that has been loaded into the pores.⁹
26 Sailor and co-workers followed up the first thermal
27 modifications of Si surfaces with work on the photoreactivity
28 of por-Si surfaces.^{10–12} Direct patterning of crystalline Si (c-Si)
29 surfaces with adsorbed alkoxide layers by photoactivation soon
30 followed.^{13,14} Chidsey^{15–17} and Buriak^{14,18–20} extensively
31 studied the photo-initiated hydrosilylation of Si and por-Si
32 surfaces.

33 Stewart and Buriak implicated excitons in the reaction
34 mechanism.¹⁸ Sun et al.²¹ extended this mechanism by invoking
35 a surface localized valence band hole coupled to radical
36 formation and propagation. Reaction proceeds by nucleophilic
37 attack of the Si surface at the site excited by the presence of the
38 hole. In a chain reaction, this is followed by H abstraction from
39 a neighboring site that allows for radical propagation.

40 Experiments consistent with the involvement of photo-
41 generated holes to enhance reactivity of Si–H bonds on both
42 extended surfaces and nanoparticles have been performed by a
43 number of groups.^{22–25} However, controversy still exists
44 regarding the details of the mechanism and how the reactivity
45 of the holes can be enhanced. Huck and Buriak²⁰ have found
46 that for white light illumination the addition of oxidants
47 possessing an acceptor level can enhance photoreactivity if the

level resides below the conduction band minimum. They
48 ascribe this to the oxidant's ability to overcome the exciton
49 binding energy.

50 Hamers and co-workers have shown that UV excitation can
51 be quite effective at grafting of terminal alkenes not only to
52 Si,^{26,27} but also to diamond and other carbon surfaces.²⁸ They
53 illuminated Ar-sparged neat alkenes in contact with a surface
54 with 254 nm light at $\sim 10 \text{ mW cm}^{-2}$. They suggested²⁶ that
55 internal photoemission is important during the grafting.
56 Internal photoemission is electron transfer from the solid
57 substrate to an acceptor species in solution by direct
58 photoexcitation. They demonstrated that this mechanism
59 works particularly well with diamond surfaces and molecules
60 that possess an acceptor level that resides below the vacuum
61 level of the solid. Huck and Buriak²⁹ found that aromatic
62 groups are particularly effective at enhancing reactivity with H-
63 terminated Si surface under 254 nm irradiation.

64 In this report, I discuss the photodynamics responsible for
65 photochemistry at Si surfaces and then develop a quantitative
66 model to fit the data of Huck and Buriak, which takes into
67 consideration both internal photoemission and electron transfer
68 in enhancing the rate of reaction. This work puts a firm
69 theoretical foundation under the suggestion in ref 26 that the
70 rate of reaction is enhanced because removal of the electron
71 from the substrate increases the lifetime of the hole that
72 initiates reactivity.

74 ■ RESULTS AND DISCUSSION

75 The initiator of UV- and visible-irradiation-induced photo-
76 chemistry by nucleophilic attack at H/Si surfaces is a
77 thermalized hole at the top of the valence band not Si–H

Received: June 19, 2013

78 bond cleavage. By conservation of energy, the Si–H bond could
79 in principle be photodissociated with a photon of wavelength λ
80 ≤ 410 nm. There are, however, no electronic transitions at this
81 wavelength. In fact, direct photodissociation of the Si–H bond
82 only begins to occur with a measurable probability at a
83 wavelength around 157 nm.^{30,31} Thermalized holes are
84 involved in the mechanism of photoinitiated etching of Si in
85 HF.^{32–34} On the basis of electronic state energetics, Kolasinski
86 has unambiguously determined³⁴ that the hole resides in a Si–
87 Si backbond bulk state localized near the surface. The hole is
88 not located in the Si–H bond, nor is it capable of dissociating
89 the Si–H bond. This state is the active state in the exciton
90 model of Stewart and Buriak.¹⁸

91 We need to consider what can influence and even enhance
92 the reactivity of the valence band hole. Foremost, the hole must
93 not recombine effectively with a conduction band electron.
94 Band bending can lead to separation of these carriers, especially
95 when only a fraction of the surface is illuminated.^{33,35} When the
96 nucleophile is strong, such as F^- , this promotes significant
97 reactivity. Hence, localized but not full surface laser excitation
98 with above band gap radiation of Si in HF(aq) leads to
99 formation of por-Si in the area that contains the holes: the
100 irradiated area of n-type Si³⁶ or the unirradiated portion of p-
101 type Si.³³ Faster and more reliable reactivity on both n- and p-
102 type wafers is induced if the hole and electron are not only
103 separated, but if the electron is completely removed from the Si
104 substrate all together. This is accomplished in stain etching in
105 which an oxidant in solution removes an electron and injects a
106 hole into the valence band.^{37–39}

107 The solid state electronic energy ϵ in electronvolts in which
108 the vacuum level is used as the energetic origin $\epsilon_{vac} = 0$ is
109 related to the electrochemical reduction potential E in volts
110 by⁴⁰

$$111 \quad \epsilon = -4.43 \text{ eV} - eE \quad (1)$$

112 The energetic origin of the electrochemical energy scale is the
113 standard hydrogen electrode (SHE) at 0 V, which has a work
114 function of 4.43 eV, and e is the elementary charge on the
115 electron. The band structure of por-Si depends on the
116 nanocrystallite size distribution because of quantum confine-
117 ment.⁴¹ For example, $E_C = -0.22$ V versus SHE and $\epsilon_{gap} = 1.12$
118 eV for 1 Ω cm p-type Si(100) in 2 M HF.⁴² However, for a
119 particular preparation of por-Si, Rehm et al.⁴³ found $E_C = -1.20$
120 V and a band gap of $\epsilon_{gap} = 2.6$ eV.

121 Excitation of electron hole pairs requiring above band gap
122 radiation requires significantly bluer photons on por-Si ($\lambda_{gap} \leq$
123 480 nm, for the visibly photoluminescent sample of Rehm et
124 al.) or sufficiently small nanocrystals of Si as compared to c-Si
125 ($\lambda_{gap} \leq 1110$ nm) because of band gap widening. Photo-
126 emission is possible once the photon energy exceeds the work
127 function. However, since Si is a semiconductor, the density of
128 states is necessarily low at the Fermi energy ϵ_F and is only the
129 result of defect states. Unless these defects are close to the
130 surface, it is unlikely that photoelectrons released from them
131 can actually leave the sample before collisional relaxation.
132 Photoelectron production occurs to a substantial extent only
133 when photons can promote electrons from the energy of the
134 valence band maximum ϵ_V . This requires ultraviolet light of λ_{VB}
135 ≤ 240 nm on c-Si or $\lambda_{VB} \leq 210$ nm on por-Si.

136 Internal photoemission removes the excited electron from
137 the Si and thereby lowers the recombination rate with the
138 valence band hole. The hole has a longer lifetime than if the
139 electron were excited to the conduction band. This intrinsically

increases the effective reactivity of the hole toward nucleophilic
140 attack by a solution phase species such as terminal alkenes.
141 Hamers and co-workers achieved a high probability for internal
142 photoemission by choosing molecules with an acceptor level
143 under the Si vacuum level and by using 254 nm light. It should
144 be noted that while charge transfer is generally most rapid to
145 the lowest energy acceptor state, internal photoemission is
146 possible not just to the lowest available state (the acceptor level
147 corresponding to the reduction potential) but to any
148 energetically accessible acceptor level.
149

To increase the hole lifetime, the excited electron must be
150 transferred to a trap state. An excited state such as $|S3\rangle$ in
151 Figure 1 is unstable and relaxes with a lifetime on the order of a
152 f

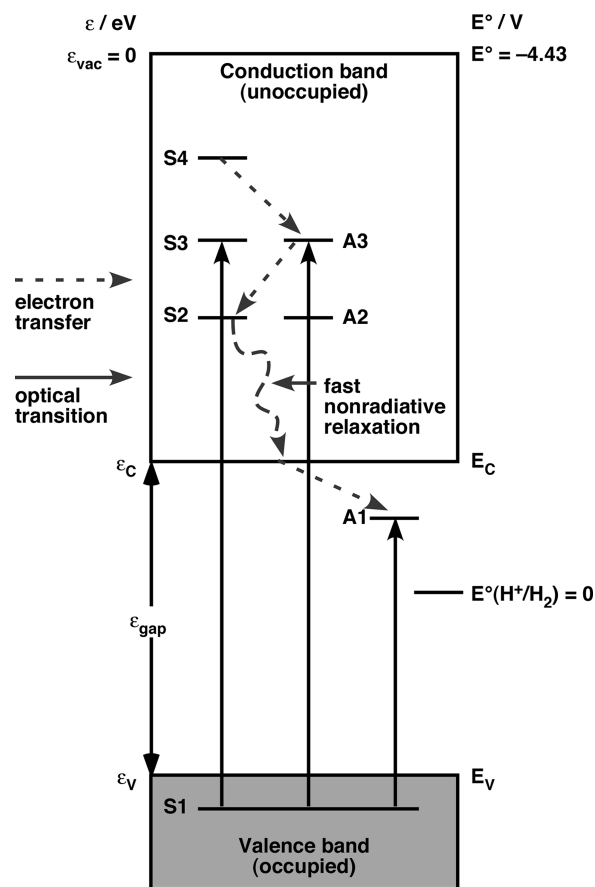


Figure 1. S1, S2, S3 and S4 represent substrate electronic states within the valence or conduction bands. A1, A2 and A3 represent molecular acceptor states in solution phase or adsorbed species.

few femtoseconds, rapidly relaxing to the conduction band
153 minimum. This is very short compared to the radiative
154 recombination time that determines the lifetime of electrons
155 at the conduction band minimum in well-passivated Si, which
156 has a lifetime on the order of a few nanoseconds to tens of
157 microseconds, depending on temperature, surface termination,
158 and nanocrystallite size.^{44,45}
159

To significantly increase the hole lifetime, the electron must
160 be transferred to a long-lived adsorbate state. Candidate states $|$
161 A1) and $|$ A3) are shown in Figure 1. As mentioned above,
162 population of these states can be accomplished by internal
163 photoemission. The rate of radiative excitation W_{fi} from initial
164 state $|i\rangle$ to final state $|f\rangle$ is given by the Fermi golden rule
165 expression
166

$$W_{\hat{n}} = \frac{2\pi}{\hbar} |V_{\hat{n}}|^2 \rho(\varepsilon_{\hat{n}}) \quad (2)$$

where the transition dipole matrix element is $V_{\hat{n}} = \langle f|\hat{\mu}|i\rangle$ and $\rho(\varepsilon_{\hat{n}})$ is the power density at the resonance energy $\varepsilon_{\hat{n}}$. The transition dipole matrix element depends on the orbital nature of the initial bulk state and the final acceptor state. Therefore, there is no reason for the internal photoemission probability to depend in a direct way on the reduction potential.

Consider two degenerate levels, one in the conduction band $|S3\rangle$ and one localized on a molecular acceptor $|A3\rangle$. There are two ways to populate the state $|A3\rangle$. The first is direct photoexcitation from a valence band state $|S1\rangle$. Whether the probability of an optical transition is greater for $|S1\rangle \rightarrow |S3\rangle$ or $|S1\rangle \rightarrow |A3\rangle$ depends on the relative magnitude of the transition dipole matrix elements $|S3\rangle|\hat{\mu}|S1\rangle$ compared to $|A3\rangle|\hat{\mu}|S1\rangle$.

The second way to transfer the electron into $|A3\rangle$ is optical excitation to $|S3\rangle$ followed by an electron transfer event $|S3\rangle \rightarrow |A3\rangle$. Here we assume that the molecules are weakly coupled (physisorbed or nonspecifically adsorbed) to the Si surface such that Marcus theory can be used to calculate the rate of electron transfer.⁴⁶

The rate of electron transfer from the conduction band can be written

$$R_{\text{inj}} = c_{\text{ox}} N_{\text{C}} k_{\text{max}} W(E) \quad (3)$$

where N_{C} is the density of states in the conduction band, k_{max} is the optimal rate constant, and $W(E)$ is the Marcus hop probability factor that depends on the relative position of the acceptor level compared to the energy of the valence band edge E_{C} . For an oxidant with Nernst potential E_{ox}

$$W(E) = \exp[-((E_{\text{C}} - E_{\text{ox}} + \lambda_{\text{e}})^2 / 4\lambda_{\text{e}} k_{\text{B}} T)] \quad (4)$$

λ_{e} is the solvent reorganization energy (about 0.5–1.5 eV for organic species at a semiconducting electrode), and k_{B} is the Boltzmann constant. k_{max} occurs when the activation Gibbs energy ΔG^{\ddagger} vanishes as defined by

$$\Delta G^{\ddagger} = (E_{\text{C}} - E_{\text{OX}} + \lambda_{\text{e}}) / 4\lambda_{\text{e}} = 0 \quad (5)$$

This condition defines the onset of the inverted region for electron transfer. Lewis and co-workers,^{47–51} have measured a value of $k_{\text{max}} \approx 10^{-25}$ to 10^{-24} $\text{m}^4 \text{s}^{-1}$ with Si, ZnO, InP, and GaAs electrodes. They have shown that this value is consistent with the maximum magnitude of k_{max} calculated quantum mechanically from

$$k_{\text{max}} = \frac{2\pi}{\hbar} |H_{\text{DA}}|^2 \beta^{-1} (4\pi\lambda_{\text{e}} k_{\text{B}} T)^{1/2} \frac{l_{\text{Si}}}{\rho_{\text{A}}^{2/3} (6/\pi)^{1/3}} \quad (6)$$

where l_{Si} is the effective coupling length in the semiconductor, $\beta \approx 1 \text{ \AA}$ is the tunneling range parameter, and H_{DA} is the coupling matrix element for the electron transfer Hamiltonian H_{et} between the donor and acceptor levels $|D\rangle$ and $|A\rangle$. The coupling matrix element H_{DA} depends on orbital overlap and symmetry. Thus, it varies exponentially with distance r from the distance of closest approach r_{m} according to

$$|H_{\text{DA}}|^2 = |D|H_{\text{et}}|A|^2 = V_0 \exp[\beta(r - r_{\text{m}})/2] \quad (7)$$

What should be apparent from Figure 1 and eqs 3–7 is that as long as $|A3\rangle$ lies above E_{C} , there always exists a state $|S2\rangle$ that lies at lower energy than $|S3\rangle$. Therefore, the activation Gibbs energy for electron transfer $|A3\rangle \rightarrow |S2\rangle$ must be less than for $|S3\rangle \rightarrow |A3\rangle$, and the rate of electron transfer out of $|A3\rangle$ must

be greater than rate of electron transfer into $|A3\rangle$. In other words, $|A3\rangle$ can never act as an electron trap state in the two-step mechanism as long as it resides above the conduction band minimum. A higher energy state such as $|S4\rangle$ could only efficiently transfer electrons to $|A3\rangle$ if the electron transfer rate were competitive with nonradiative relaxation in the conduction band, which is unlikely. $|A3\rangle$ can only act as a trap state if electron transfer to the conduction band is slow compared to the direct optical excitation rate and the rate of diffusion of the molecule away from the surface.

On the other hand, a state such as $|A1\rangle$, which resides in the band gap, can act as an effective trap state. Electron transfer from $|A1\rangle$ into the conduction band is slow because of the need for thermal activation to go back up to the conduction band at higher energy. The rate of electron transfer to the valence band is low because of the low density of empty states in the valence band.

On the basis of these considerations, I constructed a model based on photochemistry induced by two competing processes: (1) direct photoexcitation by internal photoemission and (2) charge transfer via the conduction band by electrons that have relaxed to the conduction band minimum. The rate of photochemistry is determined by the concentration of holes at the surface. Holes are produced by photoexcitation and lost by recombination. Assuming that the only holes to react are those that are made free of recombination by removal of the excited electron by direct internal photoemission or charge transfer, the yield is represented by the sum of these two contributions

$$Y(\lambda_{\text{ex}}, E_{\text{red}}, \lambda_{\text{e}}, E_{\text{C}}) = R_{\text{direct,ox}}(\lambda_{\text{ex}}) + R_{\text{inj}}(E_{\text{red}}, \lambda_{\text{e}}, E_{\text{C}}) \quad (8)$$

The rate of direct excitation of the particular oxidant ox depends on the excitation wavelength λ_{ex} . To minimize the number of parameters in the model, this rate is taken to be a constant R_{direct} . Although this may seem a severe approximation, note that a sufficiently small λ_{ex} will always be able to make a resonant transition from an appropriate initial state in the valence band and that Huck and Buriak utilized a white light source for irradiation. Monochromatic irradiation of the surface would be more likely to produce values of R_{direct} that vary from one species to the next as expected according to the resonance and density of states dependences in eq 2. Because the lifetime of electrons excited high in the conduction band is so short, $R_{\text{inj}} = 0$ for any state above the conduction band minimum ($E_{\text{red}} < E_{\text{C}}$). Therefore, the yield of species i relative to dodecene is

$$Y_{\text{rel}} = \frac{Y_i}{Y_{\text{d}}} = \frac{R_{\text{direct}} + R_{\text{inj},i}}{R_{\text{direct}}} = 1 + R_{\text{inj},i}/R_{\text{direct}} \quad (9)$$

Substituting from eq 6 and further limiting the number of parameters by assuming $k_{\text{max}} = 5 \times 10^{-25} \text{ m}^4 \text{ s}^{-1}$ and λ_{e} is the same for the solvated oxidants, a two-parameter model is obtained to fit the relative yield data of Huck and Buriak (Figure 2).²⁰ The result is an excellent fit with $R_{\text{direct}} = (5.2 \pm 1.2) \times 10^{26} \text{ m}^{-2} \text{ s}^{-1}$ and $\lambda_{\text{e}} = 1.1 \pm 0.06 \text{ eV}$. The fit was weighted by the reported experimental uncertainty and uncertainties of fit parameters are reported at 95% confidence limits.

Recall that the band gap and E_{C} depend on the nanocrystallite size. This engenders the self-limiting nature of Si etching in acidic fluoride solutions that leads to nanostructure

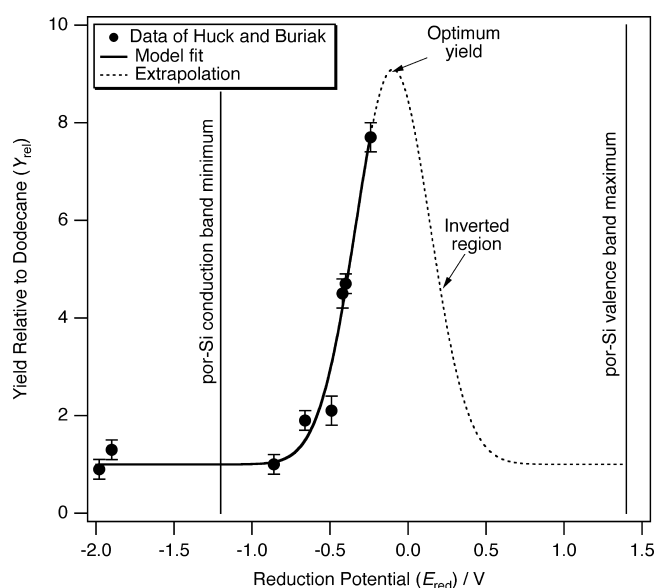


Figure 2. The result of a weighted fit of eq 9 to the data of Huck and Buriak.²⁰ The conduction band minimum and valence band maximum positions indicated are for the case of por-Si referenced in the text. After attaining the optimal rate constant, the yield is predicted to plunge in the inverted region.

formation.⁴¹ Therefore, it is possible not only to tune the rate of photoinduced electron transfer from the conduction band to [111], but also to tune this according to the size of the nanocrystalline Si object (pore wall or nanocrystal) that is in contact with the molecular acceptor level. The rate of electron transfer is tuned by choosing E_{ox} and λ_e appropriately because the optimal electron transfer rate occurs at

$$E_C - E_{ox} + \lambda_e = 0 \quad (10)$$

As noted above, the band gap of c-Si corresponds to the energy of a photon with wavelength $\lambda_{gap} = 1110$ nm, but for por-Si, $\lambda_{gap} = 480$ nm. Therefore, by choosing blue or UV light, we can excite electrons across the band gap of all nanocrystallites in a sample. Alternatively, by choosing a redder wavelength, we can preferentially excite only the larger nanocrystals.

A molecule with $E_{ox} = -0.2$ V and $\lambda_e = 1.0$ eV would accept electrons from the por-Si at the optimal rate. However, since it is resonant with the conduction band, it would be a poor trap state for c-Si. This molecule would very effectively enhance the photo reactivity of small nanocrystals but do much less to enhance the reactivity of large crystallites and flat Si surfaces.

A molecule with $E_{ox} = +0.78$ V and $\lambda_e = 1.0$ eV would accept electrons from the c-Si at the optimal rate but would lie in the inverted region for por-Si, thus accepting electrons at a much lower rate. Consequently, we can bias reactivity toward flat surfaces or larger crystallites or to smaller crystallites by choice of excitation wavelength and by choice of the acceptor molecule.

CONCLUSIONS

Internal photoemission can be quite effective at promoting photoreactivity, especially not only when the acceptor level resides in a band gap, but also when the level is strongly optically coupled to the valence band. Diamond is an exceptionally well-suited material because of its extremely wide band gap and a vacuum level positioned below the

conduction band minimum. Indeed, Hamers and co-workers^{27,28} have exploited this for efficient covalent modification of diamond and other carbonaceous surfaces. A two-step photoexcitation/charge transfer mechanism is most efficient when the acceptor level resides in a band gap, which quantitatively explains the results of Huck and Buriak.²⁰ Monochromatic excitation may lead to more complex behavior of the direct photoexcitation rate than implied in eq 9. Nonetheless, with judicious choice of the excitation wavelength, redox potential of the acceptor level and the reorganization energy of the acceptor molecule, it is possible to construct photochemical surface modification schemes that will selectively react with nanocrystalline Si.

AUTHOR INFORMATION

Corresponding Author

kkolasinski@wcupa.edu

Notes

The authors declare no competing financial interest.

REFERENCES

- Salonen, J.; Lehto, V. P. *Chem. Eng. J.* **2008**, *137*, 162.
- Salonen, J.; Kaukonen, A. M.; Hirvonen, J.; Lehto, V. P. *J. Pharm. Sci.* **2008**, *97*, 632.
- Santos, H. A.; Salonen, J.; Bimbo, L. M.; Lehto, V. P.; Peltonen, L.; Hirvonen, J. *J. Drug Delivery Sci. Technol.* **2011**, *21*, 139.
- Clark, R. J.; Dang, M. K. M.; Veinot, J. G. C. *Langmuir* **2010**, *26*, 15657.
- Ruizendaal, L.; Bhattacharjee, S.; Pournazari, K.; Rosso-Vasic, M.; de Haan, L. H. J.; Alink, G. M.; Marcelis, A. T. M.; Zuilhof, H. *Nanotoxicology* **2009**, *3*, 339.
- Canham, L. T.; Reeves, C. L.; Wallis, D. J.; Newey, J. P.; Houlton, M. R.; Sapsford, G. J.; Godfrey, R. E.; Loni, A.; Simons, A. J.; Cox, T. I.; Ward, M. C. L. *Mater. Res. Soc. Symp. Proc.* **1997**, *452*, 579.
- Bowditch, A. P.; Waters, K.; Gale, H.; Rice, P.; Scott, E. A. M.; Canham, L. T.; Reeves, C. L.; Loni, A.; Cox, T. I. *Mater. Res. Soc. Symp. Proc.* **1999**, *576*, 149.
- Canham, L. T. *Adv. Mater.* **1999**, *11*, 1505.
- Anglin, E. J.; Schwartz, M. P.; Ng, V. P.; Perelman, L. A.; Sailor, M. J. *Langmuir* **2004**, *20*, 11264.
- Lee, E. J.; Ha, J. S.; Sailor, M. J. *J. Am. Chem. Soc.* **1995**, *117*, 8295.
- Lee, E. J.; Bitner, T. W.; Ha, J. S.; Shane, M. J.; Sailor, M. J. *J. Am. Chem. Soc.* **1996**, *118*, 5375.
- Lee, E. J.; Bitner, T. W.; Hall, A. P.; Sailor, M. J. *J. Vac. Sci. Technol. B* **1996**, *14*, 2850.
- Effenberger, F.; Götze, G.; Bidlingmaier, B.; Wezstein, M. *Angew. Chem., Int. Ed. Engl.* **1998**, *37*, 2462.
- Stewart, M. P.; Buriak, J. M. *Angew. Chem., Int. Ed. Engl.* **1998**, *37*, 3257.
- Cicero, R. L.; Linford, M. R.; Chidsey, C. E. D. *Langmuir* **2000**, *16*, 5688.
- Terry, J.; Linford, M. R.; Wigren, C.; Cao, R.; Pianetta, P.; Chidsey, C. E. D. *J. Appl. Phys.* **1999**, *85*, 213.
- Terry, J.; Linford, M. R.; Wigren, C.; Cao, R.; Pianetta, P.; Chidsey, C. E. D. *Appl. Phys. Lett.* **1997**, *71*, 1056.
- Stewart, M. P.; Buriak, J. M. *J. Am. Chem. Soc.* **2001**, *123*, 7821.
- Buriak, J. M. *Chem. Rev.* **2002**, *102*, 1271.
- Huck, L. A.; Buriak, J. M. *J. Am. Chem. Soc.* **2012**, *134*, 489.
- Sun, Q. Y.; de Smet, L. C. P. M.; van Lagen, B.; Giesbers, M.; Thune, P. C.; van Engelenburg, J.; de Wolf, F. A.; Zuilhof, H.; Sudholter, E. J. R. *J. Am. Chem. Soc.* **2005**, *127*, 2514.
- Rijksen, B.; van Lagen, B.; Zuilhof, H. J. *J. Am. Chem. Soc.* **2011**, *133*, 4998.
- de Smet, L. C. P. M.; Zuilhof, H.; Sudholter, E. J. R.; Lie, L. H.; Houlton, A.; Horrocks, B. R. *J. Phys. Chem. B* **2005**, *109*, 12020.

- 378 (24) Cai, W.; Lin, Z.; Strother, T.; Smith, L. M.; Hamers, R. J. *J. Phys. Chem. B* **2002**, *106*, 2656.
- 380 (25) Holm, J.; Roberts, J. T. *Langmuir* **2009**, *25*, 7050.
- 381 (26) Wang, X. Y.; Ruther, R. E.; Streifer, J. A.; Hamers, R. J. *J. Am. Chem. Soc.* **2010**, *132*, 4048.
- 383 (27) Lasseter, T. L.; Clare, B. H.; Abbott, N. L.; Hamers, R. J. *J. Am. Chem. Soc.* **2004**, *126*, 10220.
- 385 (28) Wang, X. Y.; Colavita, P. E.; Streifer, J. A.; Butler, J. E.; Hamers, R. J. *J. Phys. Chem. C* **2010**, *114*, 4067.
- 387 (29) Huck, L. A.; Buriak, J. M. *Langmuir* **2012**, *28*, 16285.
- 388 (30) Pusel, A.; Wetterauer, U.; Hess, P. *Phys. Rev. Lett.* **1998**, *81*, 645.
- 389 (31) Vondrak, T.; Zhu, X.-Y. *Phys. Rev. Lett.* **1999**, *82*, 1967.
- 390 (32) Koker, L.; Kolasinski, K. W. *J. Phys. Chem. B* **2001**, *105*, 3864.
- 391 (33) Koker, L.; Kolasinski, K. W. *Phys. Chem. Chem. Phys.* **2000**, *2*, 392 277.
- 393 (34) Kolasinski, K. W. *Phys. Chem. Chem. Phys.* **2003**, *5*, 1270.
- 394 (35) Ashruf, C. M. A.; French, P. J.; Bressers, P. M. M. C.; Sarro, P. M.; Kelly, J. J. *Sens. Actuators, A* **1998**, *66*, 284.
- 396 (36) Noguchi, N.; Suemune, I. *Appl. Phys. Lett.* **1993**, *62*, 1429.
- 397 (37) Turner, D. R. *J. Electrochem. Soc.* **1960**, *107*, 810.
- 398 (38) Kolasinski, K. W. In *Nanostructured Semiconductors: From Basic Research to Applications*; Granitzer, P., Rumpf, K., Eds.; Pan Stanford Publishing: Singapore, 2013.
- 401 (39) Kolasinski, K. W.; Barclay, W. B. *Angew. Chem., Int. Ed.* **2013**, *52*, 6731.
- 403 (40) Kolasinski, K. W. *Surface Science: Foundations of Catalysis and Nanoscience*, 3rd ed.; Wiley: Chichester, 2012.
- 405 (41) Kolasinski, K. W. *J. Phys. Chem. C* **2010**, *114*, 22098.
- 406 (42) Gorostiza, P.; Allongue, P.; Diaz, R.; Morante, J. R.; Sanz, F. J. *Phys. Chem. B* **2003**, *107*, 6454.
- 408 (43) Rehm, J. M.; McLendon, G. L.; Fauchet, P. M. *J. Am. Chem. Soc.* **1996**, *118*, 4490.
- 410 (44) Wang, J.; Song, L.; Zou, B.; El-Sayed, M. A. *Phys. Rev. B* **1999**, *59*, 5026.
- 412 (45) Song, L.; ElSayed, M. A.; Chen, P. C. *J. Appl. Phys.* **1997**, *82*, 413 836.
- 414 (46) Kolasinski, K. W.; Gogola, J. W.; Barclay, W. B. *J. Phys. Chem. C* **2012**, *116*, 21472.
- 416 (47) Hamann, T. W.; Gstrein, F.; Brunchwitz, B. S.; Lewis, N. S. *J. Am. Chem. Soc.* **2005**, *127*, 13949.
- 418 (48) Royea, W. J.; Fajardo, A. M.; Lewis, N. S. *J. Phys. Chem. B* **1998**, *102*, 3653.
- 419 (49) Royea, W. J.; Fajardo, A. M.; Lewis, N. S. *J. Phys. Chem. B* **1997**, *101*, 11152.
- 422 (50) Fajardo, A. M.; Lewis, N. S. *J. Phys. Chem. B* **1997**, *101*, 11136.
- 423 (51) Pomykal, K. E.; Fajardo, A. M.; Lewis, N. S. *J. Phys. Chem.* **1996**, *100*, 3652.